An Examination of Radar and Rain Gauge–Derived Mean Areal Precipitation over Georgia Watersheds

Keith M. Stellman* and Henry E. Fuelberg

Department of Meteorology, The Florida State University, Tallahassee, Florida

Reggina Garza and Mary Mullusky[+]

Southeast River Forecast Center, Peachtree City, Georgia

ABSTRACT

Compared to conventional rain gauge networks, the Weather Surveillance Radar-1988 Doppler provides precipitation estimates at enhanced spatial and temporal resolution that River Forecast Centers can use to improve streamflow forecasts. This study documents differences between radar-derived (stage III) mean areal precipitation (MAPX) and rain gauge–derived mean areal precipitation (MAP). The area of study is the headwaters of the Flint River basin, specifically the Culloden basin located in central Georgia south of Atlanta, with a drainage area of 1853 mi^2. The timing of radar installations in the southeast United States provided overlapping data for only 2 yr (Jun 1996–Jul 1998). The MAP and MAPX products being examined were prepared using procedures identical to those employed operationally at the National Weather Service's Southeast River Forecast Center.

Results show that the radar (MAPX) underestimates gauge-derived rainfall (MAP) by ~38% at the end of the 2-yr period. This underestimate is most pronounced during the winter months of November–April when MAPX underestimates MAP by ~50%. Comparisons during the summer (May–Oct) indicate that MAPX is similar to MAP. The underestimation of winter rainfall likely is due to several factors: the inappropriate combination of radar values in areas of overlapping coverage, the radar beam overshooting the tops of stratiform rainfall, an inappropriate Z–R relationship, faulty radar calibration, and too few hourly rain gauges to prepare an accurate stage II bias adjustment factor and quality control the stage III product.

1. Introduction

In a typical year flooding kills more people in the United States than does any other weather phenomenon. Major efforts have been under way for several years to improve flood forecasts. Although sparse rain gauge networks and the frequency of those observations have been limitations to forecasting, more sources of data are becoming available, including observations at both greater spatial and temporal resolution. High-resolution radar-derived rainfall data from the National Weather Service Weather Surveillance Radar-1988 Doppler (WSR-88D) network may be a great advantage in river forecasting.

The National Weather Service River Forecast System (NWSRFS) is a comprehensive set of models and hydrologic techniques to simulate and/or forecast streamflow during both flooding and nonflooding conditions (Office of Hydrology 1999). Precipitation and streamflow data from various types of observing platforms are used as input to the NWSRFS. The current operational procedure utilizes a single 6-h mean areal precipitation (MAP) value over a river basin. Specifically, MAP is calculated from rain gauge data, and the resulting MAP value is used for the entire basin regardless of its size, shape, and topography.

Several recent studies have examined the use of radar-derived precipitation in streamflow forecasting. For example, 1-hourly radar-derived rainfall data from the WSR-88D were shown to increase the lead time for forecasting flash flood events over small watersheds near Pittsburgh (<200 mi^2) (Davis and Jendrowski 1993). The use of high-resolution radar-derived rainfall data also has been investigated over river basins in Oklahoma, where radar-derived values were found to underestimate MAP by 5%–10% (Smith et al. 1999). In another study within Oklahoma, Fo et al. (1998) determined that radar-derived rainfall underestimated gauge-

* Current affiliation: Lower Mississippi River Forecast Center, Slidell, Louisiana.

[+] Current affiliation: Hydrologic Research Laboratory, Washington, D.C.

Corresponding author address: Henry E. Fuelberg, Department of Meteorology, The Florida State University, Tallahassee, FL 32306-4520.
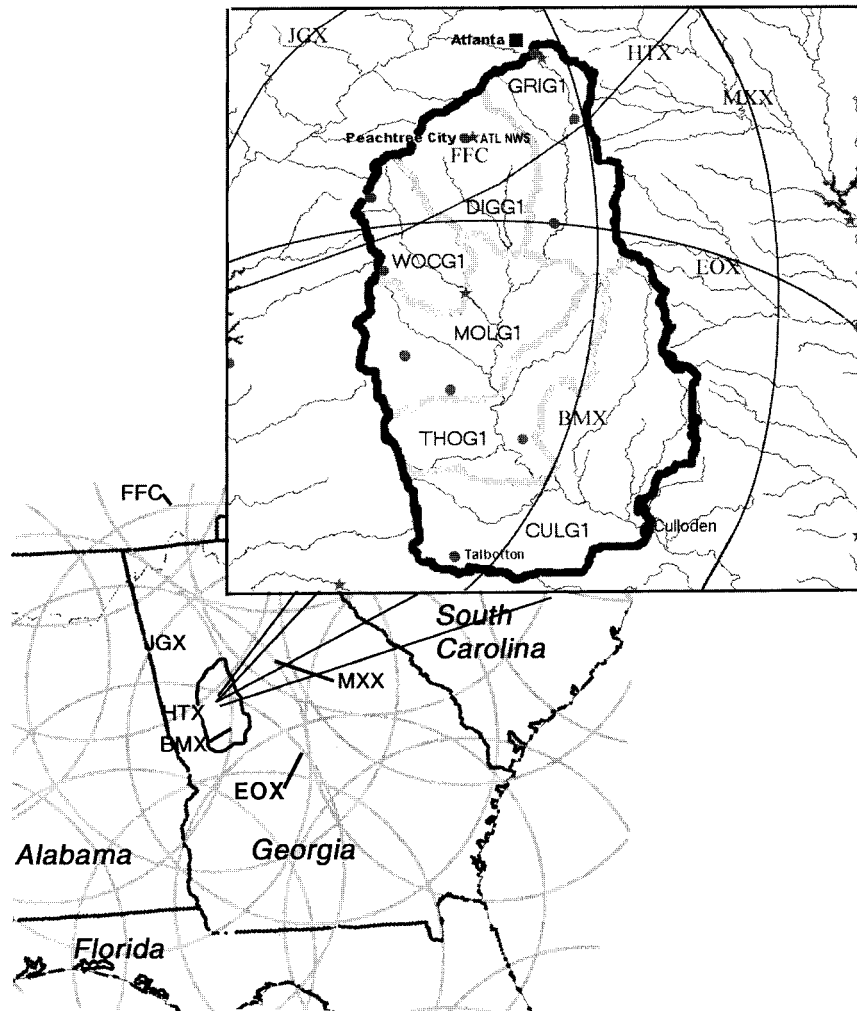E-mail: fuelberg@met.fsu.edu

Fig. 1. The Culloden basin in central Georgia is outlined in black (CLUG1), with the six subbasins outlined in gray. Twelve daily rain gauges (circles) and six-hourly rain gauges (stars) are used to generate MAP. Coverages from the six radars (labeled) that encompass the basin are shown (125 n mi range rings). Radar coverage over the southeast United States and the CLUG1 basin also is shown.

derived rainfall by ~40% when compared on a point precipitation basis. Both of these studies utilized data from the Oklahoma mesonetwork as ground truth. Klazura et al. (1999) compared radar–gauge pairs at many locations across the country, separating cases with high reflectivity gradients (convective precipitation) from those with weak reflectivity gradients (stratiform precipitation). Results showed that values from gauges and radars were nearly equal during convective rainfall situations, but gauge values were approximately double the radar-derived values during low reflectivity gradients. Thus, radar-derived stratiform rainfall was underestimated by ~50% in most regions of the country. Other studies that have compared radar and rain gauge–derived rainfall also have documented large discrepancies between the two (e.g., Baeck and Smith 1998; McGregor et al. 1995; Woodley et al. 1975).

The National Weather Service River Forecast Centers (RFCs) soon will utilize radar-derived precipitation in their streamflow models. Therefore, it is important to evaluate the radar data and, if necessary, consider ways to improve them to best represent the true rainfall over a basin. The current study analyzes radar-derived mean areal precipitation (MAPX) and rain gauge–based mean areal precipitation (MAP) over the Culloden basin (CLUG1) in central Georgia (Fig. 1). The Culloden basin was selected due to its large size (1853 mi^2), diverse topography, land use that includes urban areas in the north and rural areas in the south, and its large economic impacts due to flooding downstream. The basin is located within the operational domain of the Southeast River Forecast Center (SERFC). MAP and MAPX also were evaluated over smaller subbasins within the Culloden basin (Fig. 1). We calculated MAP and MAPX
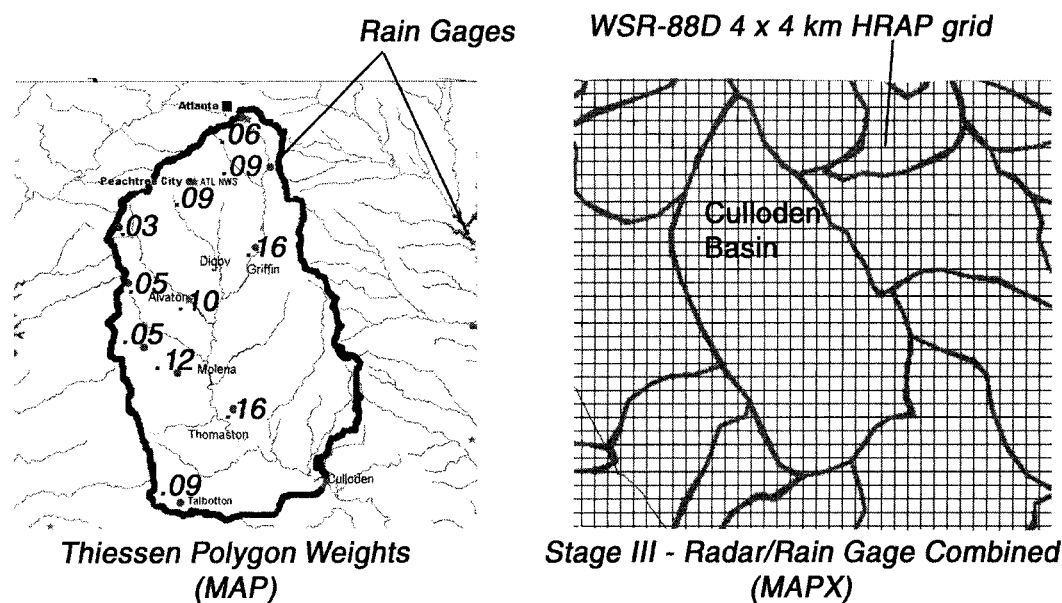
FIG. 2. (left) Thiessen polygon weights for each rain gauge used in computing MAP for the Culloden basin. (right) HRAP grid overlayed on the CLUG1 basin.

using operational procedures that are employed daily at the SERFC. Our objective is to determine whether seasonal biases exist in these operational products. To our knowledge, this is the first study to compare MAPX with MAP over the southeast United States for an extended period.

2. Data and methodology

a. Mean areal precipitation

Since most WSR-88D radars in the southeast United States were commissioned during the mid-1990s, we only could examine the period June 1996 through July 1998. The gauge data that were used to calculate MAP were gathered from the archives of several organizations, including the SERFC, National Climatic Data Center, and Forecast Systems Laboratory. The data had been quality controlled by the respective archiving agency. Data from all types of gauges were included, for example, tipping bucket, manual, weighing. These data have not yet been added to the NWS Office of Hydrology database.

A major source of error in gauge measurements is from turbulence and increased winds around the gauge. Errors in areal measurements from gauges are most prominent when the rainfall field has substantial spatial variations. Wilson and Brandes (1979) discuss these issues in detail.

The river forecast model requires 6-hourly data (Office of Hydrology 1999). Therefore, both hourly and daily rain gauge data were used in the MAP calculations, with the hourly data used to distribute (i.e., interpolate) the daily values into the proper 6-h period. This temporal distribution is performed by calculating the inverse of the distance squared between each daily gauge and hourly gauge. Since hourly data are scarce, sites slightly outside the basin were used in addition to sites within the basin (Fig. 1).

MAP can be calculated within NWSRFS using several different procedures. We used the Thiessen polygon method (Viessman and Lewis 1996) in this study since it is used operationally at the SERFC. The Thiessen method divides a basin into polygons based on gauge locations and distances between gauges (Office of Hydrology 1999). The polygon surrounding each rain gauge represents an area that becomes a weighting factor describing how that gauge contributes to the total basin MAP (Chow et al. 1988). Figure 2 shows the Thiessen weights for each of the 12 gauges that were used to compute MAP within the Culloden basin. Only sites within the basin were used in the Thiessen calculations, and if daily and hourly gauges were collocated, only one was utilized.

b. Radar mean areal precipitation

We calculated MAPX using operational products and procedures employed by the RFCs to derive precipitation from radar data. Since these techniques are described in detail by Fulton et al. (1998), Seo (1998a,b), and Seo et al. (1999), only highlights are given here. During stage I of the process, the individual NWS Forecast Offices produce the hourly digital precipitation (HDP) product. During our study period, the NWS offices usually used the standard Z–R relationship $(300R^{1.4})$ for this purpose; however, during tropical sit-

uations, some radars may have switched to the tropical Z–R relation ($250R^{1.2}$). HDP is mapped on a polar stereographic projection called the Hydrologic Rainfall Analysis Project (HRAP) grid, having a spatial resolution of approximately 4 km $\times$ 4 km. Figure 2 shows the HRAP grid over the Culloden basin. The stage I product that is generated at each local radar site is transferred to the RFC.

During the stage II process, the RFC combines the hourly radar product (stage I) with hourly rain gauge data to make a composite radar–rain gauge image for each radar site. This compositing is performed using multivariate objective analysis. Specifically, each gauge-derived rainfall value is compared with radar-derived values at the gauge's nine closest (i.e., surrounding) HRAP grid cells. The difference between the gauge value and the HRAP cells is used to compute a bias. A number of these gauge–radar pairs are used to compute the bias, with the exact number set locally at the RFC. However, the minimum number of pairs is three. This bias is applied each hour over the entire radar coverage area until a new set of gauge–radar pairs is available (Smith and Krajewski 1991; Anagnostou et al. 1998; Seo et al. 1999). For example, if there are three gauge–radar pairs (excluding zero values) under a radar umbrella during a given hour, then the three biases are averaged, with the result applied to the radar's entire area of coverage. If there are fewer than three gauge–radar pairs for a given hour, the bias from the previous hour is applied to the entire area.

If radar data are missing for a particular hour, then each gauge under that radar's umbrella is assigned a radius of influence that has been predetermined through a trial and error process. This gauge influence radius typically is two to three HRAP bins. For example, if a gauge reports rainfall for a given hour when the radar data are missing, the result is a circle of rainfall having a maximum at the gauge site. Conversely, if radar data are available, but indicate rainfall over a gauge that reports zero, then an HRAP bin of zero would exist among positive radar values. The end product of this process is called stage II.

Stage III, the third stage of processing, combines the individual stage II products from the various radars within the RFC's area of responsibility into a single mosaic. During this procedure, the stage II products are quality controlled to remove any erroneous gauge or radar data due to anomalous propagation, ground clutter, or bright banding. The RFC has the choice of not using a specific radar if it is known to greatly overestimate or underestimate rainfall. In areas of overlapping radar coverage, the multiple values at a given HRAP grid point either can be averaged, or the maximum value can be used. This determination is made by the individual RFC. During our study period, values were averaged by the SERFC, following guidelines of the Office of Hydrology. The final quality controlled mosaic representing the combination of several stage II products is called stage III.

Finally, the RFC uses the stage III product to compute basin-averaged precipitation—denoted MAPX. MAPX is simply the sum of the precipitation values at each stage III grid cell within the predefined basin divided by the number of cells within that basin (Fig. 2). We used the operationally derived stage III products from the archive of the SERFC in the current study, calculating MAPX using the standard RFC software for that purpose.

Several initial points should be made regarding the MAPX data used in this study. Since the Culloden basin mostly is located in a sparsely populated region of central Georgia, only three hourly gauges within the basin's boundaries were available to quality control the hourly stage III radar–rain gauge composite (Fig. 1). Another limitation is that one or more of the radars used to prepare MAPX may have been miscalibrated at some time during the study period. Finally, it should be noted that additional radars have been added through the years, thereby changing the number of values that could be averaged in areas of overlapping radar coverage.

Values of MAP were calculated at 6-h intervals between 1 June 1996 and 31 July 1998, while MAPX was computed at 1-h intervals and then summed to 6-h intervals during that same period. Although MAPX could have been used as a 1-h time series, the 6-h interval facilitated a direct comparison with MAP. Computations were made for both the entire (lumped) Culloden basin and for six subbasins (Fig. 1) that were used in a semidistributed streamflow simulation (see Stellman et al. 1999). This subdivision was based on the availability of streamflow and channel data at the outlet of each subbasin from the United States Geological Survey (USGS). Most previous studies that compared rain gauge data with radar-derived data were conducted over Oklahoma where there is a mesonetwork of gauges, for example, Fo et al. (1998), Smith et al. (1999), and Klazura et al. (1999). However, a dense mesonetwork is not available over most of the United States, including the southeast.

3. Results

a. Entire period

Means and standard deviations of MAP and MAPX over the lumped CLUG1, as well as the linear correlation between these quantities over 6-h rain periods, are shown by month in Fig. 3. The results show a definite seasonal bias, with MAPX underestimating MAP by as much as 60% during February. Conversely, agreement during the summer months is much better. Specifically, MAPX indicates somewhat more rainfall than MAP during the months of June and July, with almost equal rainfall in May. During the other summer months of
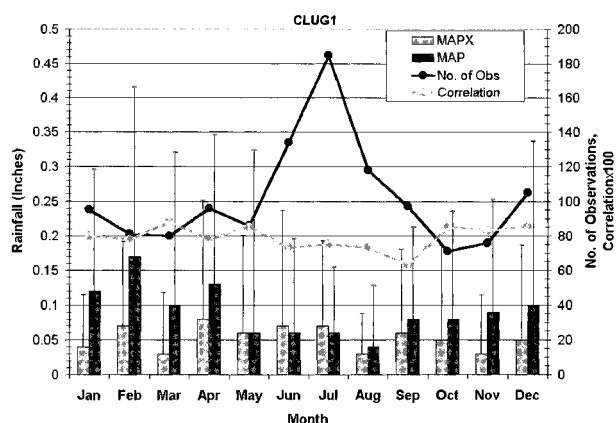
FIG. 3. Mean rainfall (in.) by month for CLUG1 for Jun 1996–Jul 1998 with standard deviations, number of 6-h periods that either method reported rainfall, and linear correlation (×100) between MAP and MAPX if either method reported rainfall.
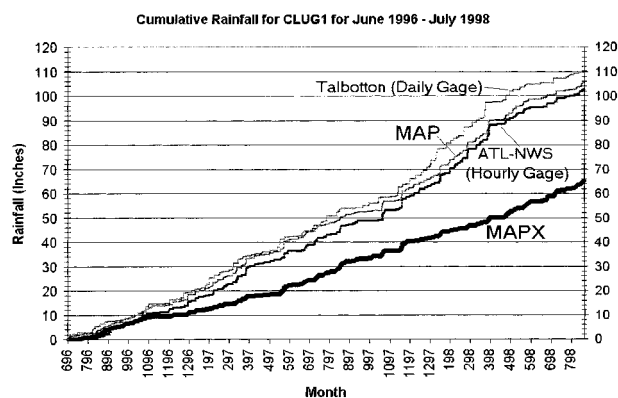

FIG. 4. Cumulative sum of MAPX and MAP for CLUG1, the Atlanta NWS hourly rain gauge data, and the Talbotton daily rain gauge data over the 2-yr period from Jun 1996 through Jul 1998. Locations of the two gauges are shown in Fig. 1.

August, September, and October, mean MAP and MAPX are within ~25% of each other.

Figure 3 also indicates that highest correlations between MAP and MAPX occur during the winter months when differences in amount are greatest. Winter month correlations are ~0.8–0.9; however, correlations of only 0.65–0.75 occur during the summer months when rainfall amounts are more similar.

The higher winter correlations (lower summer correlations) likely are due to MAP and MAPX indicating rainfall during the same (different) 6-h periods. That is, when both methods consistently indicate rainfall during the same 6-h period, correlations between them will be higher than if the rainfall is indicated in different periods. The time and duration of precipitation determined by radar may disagree with those determined from the mostly daily gauge data that were temporally distributed (interpolated) by the few hourly gauges. As a result, the timing of operational MAP is less reliable than the timing of MAPX (Seo and Smith 1996; Smith et al. 1996). The greatest differences in timing are expected with warm season, mostly convective rainfall, due to its smaller spatial and temporal scale. Even though amounts of MAPX and MAP do not agree closely during the winter months (Fig. 3), both methods generally indicate some rainfall within the same 6-h period, explaining the higher correlations. This timing of rainfall hypothesis will be illustrated in sections 3b and 3c when individual cases are examined.

Standard deviations of rainfall also exhibit a seasonal bias (Fig. 3). Specifically, standard deviations of MAP are greater during winter than summer, indicating that MAP is more variable during winter. Although patterns of convective precipitation that dominate the summer are more spatially and temporally variable than those of the more stratiform winter precipitation, the range of MAP is greatest during winter. The MAPX data do not exhibit this enhanced winter variability. However,

MAPX does exhibit greater standard deviations than MAP during some summer months. This may be due to the variability in convective rainfall totals, which are better represented by the radars than the sparse rain gauges.

Figure 4 shows the cumulative sum of 6-h MAP and MAPX for the lumped Culloden basin over the 2-yr period. The graph also includes sums from the Atlanta NWS hourly rain gauge and the Talbotton daily gauge (see locations in Fig. 1). These two sites were selected because they contained no missing data during the 2-yr period. Gage values at the end of the period are 102 in. and 109 in. for the hourly and daily site, respectively. MAP at the end of the period is ~106 in. while the MAPX sum is ~66 in. Thus, MAPX is ~40 in. less than MAP, corresponding to an overall 38% underestimate.

A careful examination of Fig. 4 reveals seasonal differences and differences between individual events. For example, near the beginning of the period (Jun 1996–Oct 1996), the cumulative sum of MAPX closely resembles that of MAP and the two gauges, indicating that rainfall during summer 1996 is depicted similarly by the two schemes. However, during the winter of 1996, the slope of the MAPX line becomes much flatter than those of the other three sources, indicating underestimation of winter rainfall. Another notable feature is the near vertical slopes of the gauge profiles during March 1998 that is less apparent in MAPX. This March event is the largest rain/flood event of the 2-yr period; it is examined in detail later in this section.

Results for the six subbasins (Fig. 1) are examined next to determine whether basin size influences observed differences between MAP and MAPX. Figure 5 shows mean rainfall for all 6-h periods when either MAP or MAPX reported rainfall. The graph shows that MAPX underestimates rainfall in every basin regardless of its size and that linear correlations decrease as basin size decreases. This decreasing correlation may be due
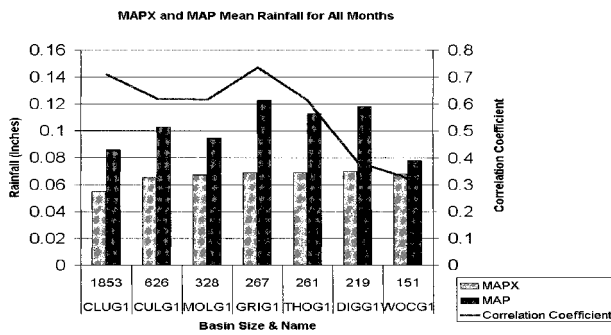
FIG. 5. Mean rainfall (in.) for all periods when either MAP or MAPX reported rainfall. Data for the lumped basin and each subbasin are given. Also shown is the basin size (mi^2) and linear correlation between MAPX and MAP when either method reported rainfall. Locations and identifiers of the subbasins are given in Fig. 1.
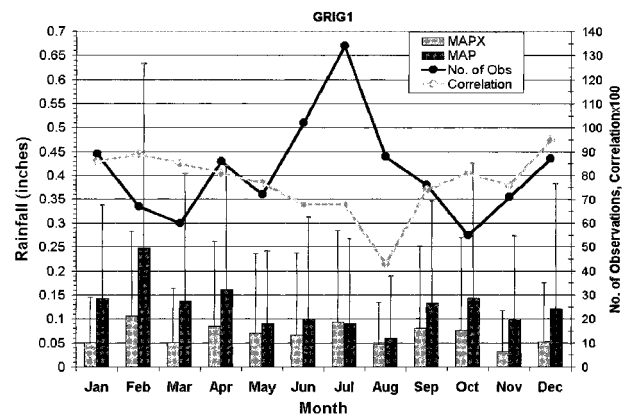

FIG. 6. Mean rainfall (in.) by month for GRIG1 for Jun 1996–Jul 1998 with standard deviation, number of 6-h periods that either method reported rainfall, and linear correlation ($\times$100) between MAP and MAPX if either method reported rainfall.

to the greater influence that the fewer rain gauges have on MAP calculations as basin size becomes smaller. That is, with fewer rain gauges to distribute rainfall into periods and calculate the basin average MAP, the correlation between MAP and MAPX decreases.

Since the subbasins contain fewer rain gauges for MAP calculations than the complete basin, we hypothesized that MAPX's enhanced horizontal resolution would be especially useful there. To explore this hypothesis, the Griffin subbasin (GRIG1, Fig. 1), located in the northern part of the Culloden basin, is examined in detail. GRIG1 was selected because it contains one hourly and three daily rain gauges, more than the other five subbasins, and because its size (267 mi^2) is nearest the average of the subbasins. GRIG1 is located within a 15–45-mi radius of the Atlanta NWS radar (Fig. 1). In spite of its proximity to Atlanta, range bias still is a factor since the basin is located within the coverage of five additional radars (Fig. 1), and the radar-derived precipitation values from all six sites were averaged to produce the stage III product in this area of overlapping coverage.

Figure 6 shows mean rainfall during all 6-h periods when either MAP or MAPX reported rainfall. Results show that differences in mean rainfall amounts, standard deviations, and linear correlations between MAP and MAPX for GRIG1 tend to be greater than those of the complete CLUG1 basin (Fig. 3) due to the smaller size of GRIG1. However, the general findings are consistent with those of the lumped basin (Fig. 3). Specifically, the seasonal bias again appears prominently; that is, MAPX greatly underestimates MAP during winter months but values are more similar during summer, although correlations between them are smaller.

Smith et al. (1999) found that MAPX was 5%–10% smaller than MAP over northeast Oklahoma during a 3½-yr period, and their biases in MAPX also changed seasonally. However, unlike current findings, their MAPX values were less than MAP during the summer season (May–Oct) rather than the winter season. Smith et al. (1999) noted that this was "the most puzzling

finding of the study since it is contradictory to current theory which generally indicates that the radar should more drastically under predict precipitation in typical winter storm systems." They concluded that the small winter bias between MAP and MAPX was due to bright banding, and because personnel at the Arkansas Basin River Forecast Center switched to the gauge-only field when processing WSR-88D data. This switch to gauge-only data meant that the stage III product was created from measured rain gauge data without the radar measurements.

The following sections compare MAP and MAPX for two seasonal categories. Specifically, winter months include November through April, while summer months include May through October. This seasonal categorization permits a detailed examination of the more stratiform (winter) rainfall and the more convectively active warm season. Additional monthly subdivisions show individual events, the timing of rainfall for each method, and differences between summer and winter rainfall.

b. Summer (convective) comparisons

Cumulative totals of MAP and MAPX over the lumped Culloden basin are shown for July 1997 and July 1998 in Figs. 7a and 7b. These two months contain the greatest summer precipitation. Figure 7 indicates that rainfall amounts from MAP and MAPX exhibit good agreement. For example, at the end of July 1997 (Fig. 7a), both cumulative amounts are ~5.5 in. Results for July 1998 (Fig. 7b) also show relatively small differences. Although these graphs and others (not shown) indicate that MAPX estimates of convective rainfall are similar to those of MAP, there usually are differences in the timing of each rainfall occurrence. Examples of this contrasting timing occur on 1, 7, 12, 27 July 1997 and 3, 8, and 12 July 1998. As previously mentioned, we believe that these differences in timing led to the lower correlations between MAP and MAPX during
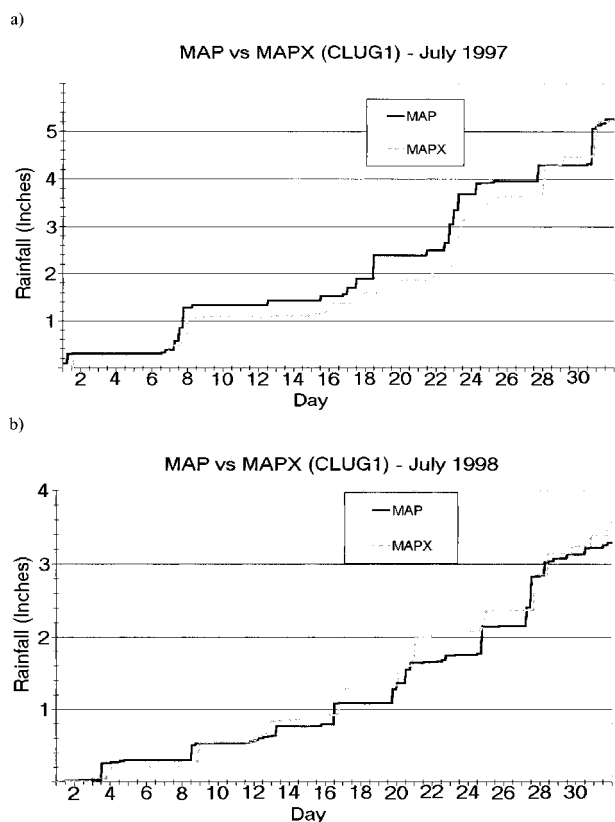
a)

MAP vs MAPX (CLUG1) - July 1997

b)

MAP vs MAPX (CLUG1) - July 1998

FIG. 7. Cumulative rainfall amounts from MAP and MAPX over CLUG1 during (a) Jul 1997 and (b) Jul 1998.

a)

MAP vs MAPX (GRIG1) - July 1997

b)

MAP vs MAPX (GRIG1) - July 3-5 1998

FIG. 8. Cumulative rainfall over GRIG1 from MAP and MAPX for (a) Jul 1997 and (b) 3–5 Jul 1998.

summer. MAPX data are expected to provide superior timing, that is, within ~1 h, versus ~6–12 h from the rain gauges.

Figure 8a shows cumulative rainfall during for the Griffin subbasin during July 1997 (GRIG1, Fig. 1). Results are similar to those for the entire basin (Fig. 7); that is, MAPX and MAP produce similar rainfall amounts but often exhibit differences in timing. These results for July 1997 are similar to those of most warm season months (not shown).

We examined individual rainfall events in detail to determine how MAP and MAPX depict rainfall amount and its timing. Figure 8b shows an event between 3 and 5 July 1998 (MAPX is plotted at hourly intervals, i.e., before summing to 6-h intervals). At the end of the period, MAPX estimates 0.65 in. of rainfall while MAP indicates 0.5 in. However, one should note that the timing of the rain periods is not similar. For example on 3 July, MAP reports the greatest rainfall between 1200 and 1800 UTC; however, MAPX reports the greatest rainfall during the next 6-h period, that is, between 1800 and 0000 UTC. Smaller differences in timing occur on 4 and 5 July (Fig. 8b). Results for the other five subbasins are similar to those shown here.

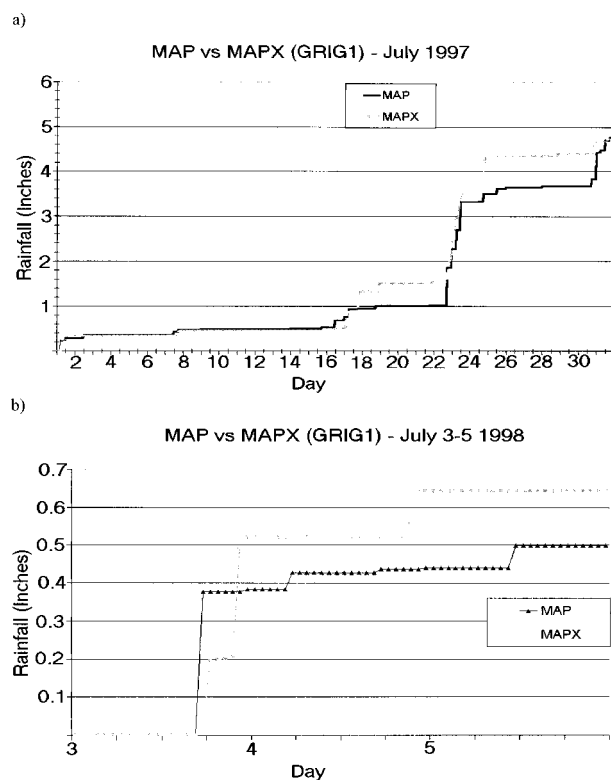Mean values and linear correlation coefficients between MAP and MAPX are shown in Fig. 9 for the lumped basin (CLUG1) and each subbasin for the combination of all summer months during the June 1996–July 1998 period. Rain events are defined as 6-h precipitation greater than 0.01 in. for either MAP or MAPX. The bar graphs show that means of the two methods generally are similar in the subbasins, within ~10% of each other. Correlation coefficients for the larger subbasins are between 0.6 and 0.7; however, values decrease with basin size.
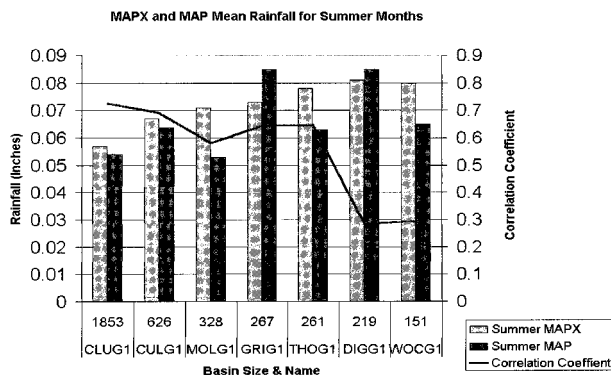
MAPX and MAP Mean Rainfall for Summer Months

FIG. 9. Mean summer rainfall (in.) for all periods when either MAP or MAPX reported rainfall. Data for the lumped basin and each subbasin are given. Also shown are the basin size (mi^2) and linear correlation between MAPX and MAP when either method reported rainfall. Locations and identifiers of the subbasins are given in Fig. 1.

a)

MAP vs MAPX (CLUG1) - December 1996

b)

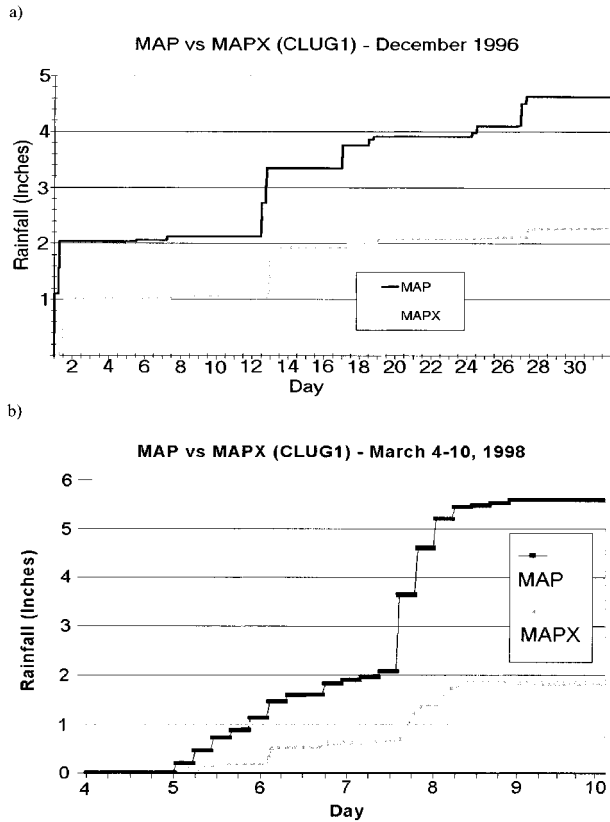**MAP vs MAPX (CLUG1) - March 4-10, 1998**

FIG. 10. Cumulative rainfall from MAP and MAPX over the lumped Culloden basin for (a) Dec 1996 and (b) 4–10 Mar 1998.

To summarize, it is clear that the 38% overall underestimation of MAPX (Fig. 4) is not attributable to summer rainfall. The winter season is examined in the following section.

c. Winter (stratiform) comparisons

Comparisons between MAP and MAPX during the winter months (Nov–Apr) employ the same techniques used for the summer months. December 1996 had the most rain days during the 2-yr period, and cumulative totals for the lumped Culloden basin during that period (Fig. 10a) show that MAPX underestimates MAP by ~50%. A close examination shows that both methods detect rainfall on 13, 17, 19, 25, and 27 December 1996, and with similar timing; however, MAPX underestimates each event. As previously noted, we believe that this similarity of timing explains the high correlations between MAP and MAPX even though the means are very different. In addition, the mainly stratiform precipitation typically has smaller spatial gradients that even a sparse gauge network can adequately sample.

A case of strong isentropic lift over the Culloden basin during the week of 4–10 March 1998 illustrates the extent to which the radar can underestimate stratiform rainfall (Fig. 10b). The MAPX total is only ~2

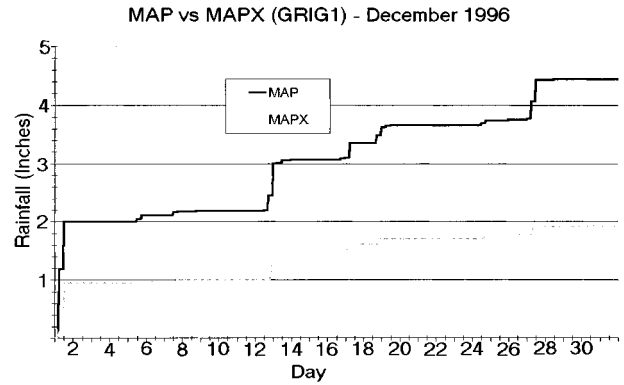**MAP vs MAPX (GRIG1) - December 1996**

FIG. 11. Cumulative rainfall from MAP and MAPX over GRIG1 for Dec 1996.

in. during the period, whereas MAP totals ~6 in. Although MAP and MAPX exhibit relatively similar timing of the rainfall, MAPX greatly underestimates the rainfall total. This major underestimate would significantly affect a flood forecast based on MAPX data.

MAPX also underestimates winter rainfall in the individual subbasins. For example, rainfall over the GRIG1 subbasin during December 1996 is shown in Fig. 11. Although MAPX underestimates total December 1996 rainfall by 57%, it generally detects rainfall within the same 6-h periods as MAP. Figure 12 shows that MAPX underestimates rainfall by 40% to 66% in the subbasins during winter months even though correlations between MAP and MAPX are as high as 0.9 for GRIG1. Although correlations tend to be somewhat lower for the smaller subbasins, this difference is not as evident as during the summer months (Fig. 9).

In summary, MAPX and MAP generally produce similar rainfall amounts during summer, but often yield different timing of individual events. Conversely, MAPX underestimates rainfall in every winter month of the 2-yr

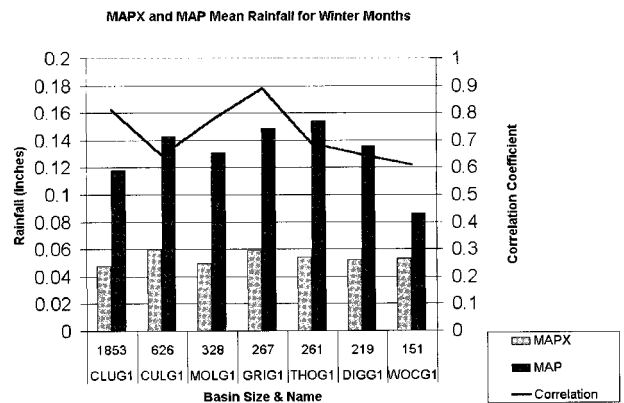**MAPX and MAP Mean Rainfall for Winter Months**

FIG. 12. Mean winter rainfall (in.) for all periods when either MAP or MAPX reported rainfall. Data for the lumped basin and each subbasin are given. Also shown is the basin size (mi²) and linear correlation between MAPX and MAP when either method reported rainfall. Locations and identifiers of the subbasins are given in Fig. 1.
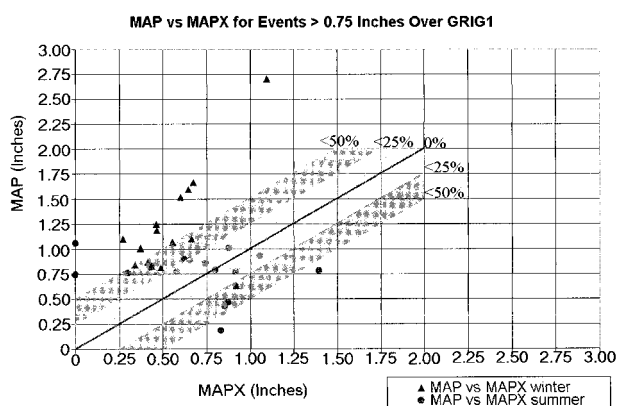
FIG. 13. MAP and corresponding MAPX values over 6-h periods for GRIG1 divided into winter and summer events with percent differences. Only cases when MAPX or MAP > 0.75 in. are shown.

period although the timing of rainfall events by MAP and MAPX is more similar during winter than summer. Differences in timing occur because MAP is based mostly on daily gauge data and because the spatial and temporal scales of winter precipitation (mostly stratiform) are greater than those of summer precipitation (mostly convective).

d. Large event comparisons

It is important to compare MAP with MAPX during heavy rain events when river response will be greatest. Figure 13 shows values of MAP and MAPX for all events greater than 0.75 in. over the GRIG1 subbasin during the 2-yr period. Results for GRIG1 are similar to those of the other subbasins (not shown). During the winter (triangles), more than half of the events exhibit a 50% or greater difference between MAP and MAPX. The MAPX rainfall exceeds MAP in only one 6-h period, and since this occurs during April, it may have been a convective event. All other winter events show MAP values exceeding MAPX from 25% to as much as 150%.

Approximately half of the summer events (circles in Fig. 13) exhibit MAP values within 25% of MAPX. In fact, all events when the difference between MAP and MAPX is smallest (0%–25%) occur during the summer. For the two summer events when MAPX reports zero rainfall, the stage III data were missing.

These event comparisons suggest that it would be impractical to use the current operational version of MAPX rainfall for streamflow simulations during the winter months because the resulting simulations would be much less than those from MAP data.

e. Case study

An event containing both stratiform and convective rainfall is shown in Fig. 14. The diagram depicts the 24-h final stage III product (radar–rain gauge composite) generated by the SERFC for 14 March 1999. It is an example of the composite product used to generate MAPX that was described in the methodology section. The radar–rain gauge gridded estimate of rainfall is superimposed on 24-h rain gauge totals (numbers in black). Although the date of this image is outside our study period, it was created using operational procedures similar to those used during our period.

The meteorological setting on 14 March included a warm frontal boundary extending across southern Alabama and the Florida–Georgia border. In the convective rainfall region over the Florida panhandle and south Georgia (Fig. 14), the stage III estimate includes areas of 4.0 in. that match closely the gauge values. However, north of the warm front, in the stratiform precipitation regions of central Alabama and west-central Georgia, stage III estimates range from 0.25 to 1.25 in., whereas gauge values are much larger, ~2 in. This image illustrates the radar's underestimation of stratiform precipitation. We believe that the contrasting depictions of stratiform versus convective precipitation lead to the seasonal biases that were described earlier.

4. Summary and conclusions

This research has documented characteristics of operational precipitation products used by the National Weather Service River Forecast Centers. Specifically, radar-derived mean areal precipitation in a river basin was compared to rain gauge-derived mean areal precipitation. The headwater of the Flint River in central Georgia, known as the Culloden basin (Fig. 1), was selected due to its large size, diverse land use, typically sparse rain gauge network, and influence on important areas downstream. The basin was separated into six subbasins based on USGS data at outlet points of each subbasin. The period of study was June 1996–July 1998.

MAP was computed from the combination of hourly and daily rain gauge data. The hourly gauges were used to distribute the daily rainfall amounts throughout the day, which then were used to create 6-hourly values of MAP over the Culloden basin. MAPX was obtained from the combination of radar-derived rainfall estimates and rain gauge data, yielding a product called stage III at ~4 km × 4 km grid spacing. The stage III product had been prepared by the Southeast River Forecast Center. We used this operational product to generate a time series of basin and subbasin MAPX at 6-h intervals.

Results for the summer months (May–Oct) showed that MAP and MAPX indicated similar amounts of rainfall, regardless of subbasin size. Conversely, results for the winter months (Nov–Apr) indicated that MAPX underestimated MAP by ~50%. Correlations between MAP and MAPX were found to be the highest during winter months. A case from March 1999, which included both convective and stratiform rainfall, illustrated the differences in detecting these types of precipitation. Specifically, stratiform precipitation amounts
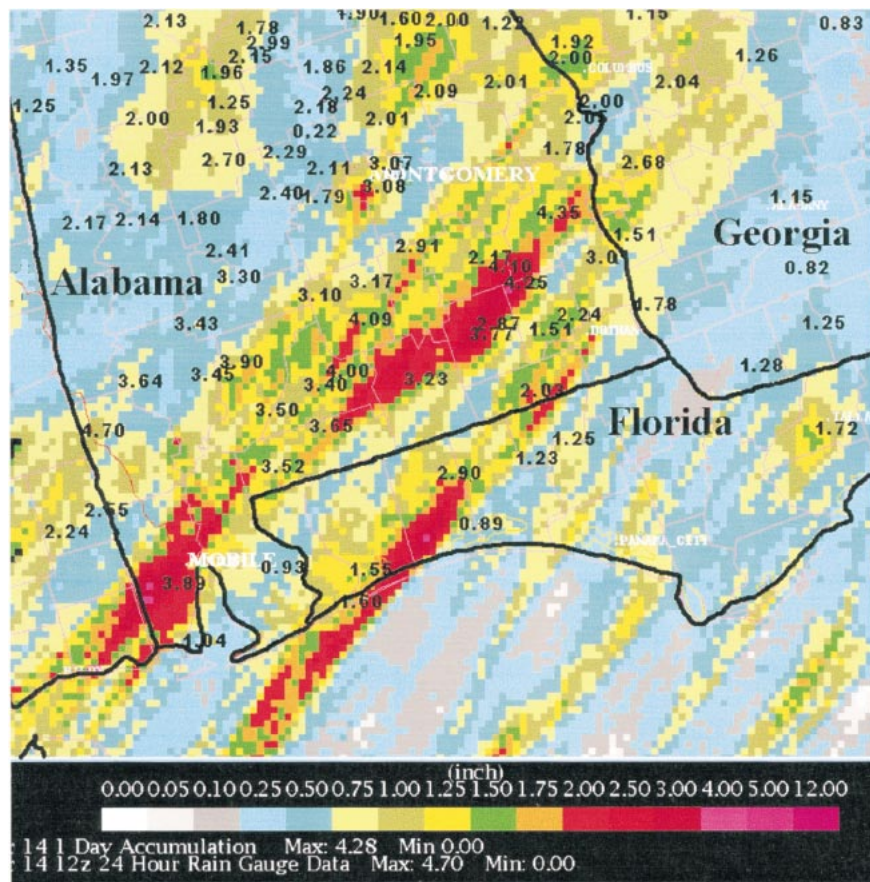
Fig. 14. Composite 24-h radar-derived rainfall on 14 Mar 1999 showing both stratiform and convective rainfall regions (see color bar). Rain gauge data are overlaid (numbers in black). This is the final stage III product.

were underestimated greatly by the radar, while the convective amounts were appropriately depicted.

Previous studies have described several factors leading to inaccuracies in radar-derived rainfall estimates. These include bright banding, beam filling, calibration errors, range effects, inappropriate Z–R relationships, attenuation, anomalous propagation (AP), ground clutter, and the sampling strategy used by the radar (e.g., Austin 1987; Fo et al. 1998; Klazura et al. 1999). Stage III techniques such as bias adjustment and averaging of overlapping radar bins also are possible sources of error. It is not possible to determine which of these factors played the greatest role on day-to-day rainfall estimates in the Culloden basin. However, since the RFC quality controls the hourly rain gauge and radar data, the AP, ground clutter, and bright banding could be removed from the final product.

Beam filling tends to be a problem during cases of strong reflectivity gradients associated with convective events. Thus, it would not explain the winter rainfall deficit shown in this study. Previous studies also have shown that rainfall is poorly estimated at the fringes of radar coverage (e.g., Fo et al. 1998; Fulton et al. 1998);

that is, the radar beam overshoots the cloud layer. However, additional radars were added to the stage III product during our study period, and there now are several radars near the Culloden basin plus one radar inside the basin.

The radar's sampling strategy also is an important factor in estimating rainfall. The two main precipitation scanning modes are Volume Coverage Pattern 11 (VCP 11), which scans 14 levels in 5 min, and VCP 21, which scans 9 levels in 6 min, thereby giving a longer listening time and thus a longer range. Although VCP 11 is the best strategy for estimating precipitation because it samples more levels, it is seldom used because of its range limitation.

The Z–R relation is a possible source of error in radar-derived rainfall estimates. Brandes et al. (1999) concluded that variations in Z–R relationships exist due to variations in drop size distributions. In addition, Ulbrich and Lee (1999) recently concluded that miscalibration of the radar contributed to errors in rainfall estimates in South Carolina. We believe that both of these factors are important contributors to the current differences between MAP and MAPX. In light of the importance of

employing the appropriate Z–R relation, National Weather Service field offices recently began using separate Z–R equations for stratiform and convective rainfall.

During our study period, the SERFC and other RFCs averaged radar-derived precipitation values in areas of overlapping coverage. Recent findings indicate that this averaging is not the optimum choice during the cool season when shallow stratiform rainfall dominates (e.g., Fo et al. 1998; Joss and Lee 1995; Viginal et al. 1999; Young et al. 1999). In addition, rainfall estimates near a particular radar site may be compromised during any season by averaging with estimates from more distant sites. We believe that this averaging process is a major source of the observed differences between MAP and MAPX during the cool season. The Lower Mississippi River Forecast Center (LMRFC) recently began using the maximum rainfall value in areas of radar overlap. Future analyses of these data will determine whether the averaging technique contributes considerably to the underestimation that was found in this study.

The Office of Hydrology soon will launch a new software program, called RFC-Wide, to compute stage III rainfall (Seo et al. 2000). RFC-Wide will utilize radar climatologies to determine at each site the areas of beam blockage and the maximum useful range. In locations of overlapping coverage, the HRAP cell from the radar having the lowest elevation will be selected. There also will be an option to use summer and winter climatologies since maximum ranges may vary with season. RFC-Wide is expected to provide improved estimates of radar-derived precipitation.

Current results suggest several recommendations for policy makers and the meteorologists and hydrologists at the RFCs:

1) Install additional hourly rain gauges in areas currently devoid of ground truth so that radar biases can be computed better.
2) Use MAPX for streamflow simulations during convective events (summer) since MAPX provides better spatial and temporal distribution of rainfall than does MAP.
3) Use MAP for streamflow simulations during winter stratiform events.
4) Increase the radius of influence of rain gauges during the winter months to improve the stage II product since rainfall typically is relatively uniform during winter.
5) Evaluate the new Z–R relationship for use during stratiform rainfall.
6) Compare MAP and MAPX in other regions of the country to confirm current results.
7) Closely monitor the radar–gauge bias so any bias is not used for an extended period.
8) Compare raw radar fields to stage II data to determine if and how much the biases improve overall rainfall estimates.

9) Switch to using maximum rainfall in overlapping regions until the RFC-Wide stage III product is distributed.
10) Initiate a systematic, periodic absolute calibration program of the radar network.

Even these suggestions probably will not solve the problems with radar-derived precipitation data and their role in streamflow forecasting. However, current results do suggest that MAPX can now be used to diagnose the spatial variability of rainfall, especially during summer.

REFERENCES

Anagnostou, E. N., W. F. Krajewski, D.-J. Seo, and E. R. Johnson, 1998: Mean-field rainfall bias studies for WSR-88D. *J. Hydrol. Eng.,* **3** (3), 149–159.

Austin, P. M., 1987: Relation between measured radar reflectivity and surface rainfall. *Mon. Wea. Rev.,* **115,** 1053–1070.

Baeck, M. L., and J. A. Smith, 1998: Estimation of heavy rainfall by the WSR-88D. *Wea. Forecasting,* **13,** 416–436.

Brandes, E. A., J. Vivekanandan, and J. W. Wilson, 1999: A comparison of radar reflectivity estimates of rainfall from collocated radars. *J. Atmos. Oceanic Technol.,* **16,** 1264–1272.

Chow, V. T., D. Maidment, and L. Mays, 1988: *Applied Hydrology.* McGraw-Hill, 572 pp.

Davis, R. S., and P. Jendrowski, 1993: The operational Areal Mean Basin Estimated Rainfall (AMBER) module. Preprints, *13th Conf. on Weather Analysis and Forecasting,* Vienna, VA, Amer. Meteor. Soc., 379–383.

Fo, A. J. P., K. C. Crawford, and C. L. Hartzell, 1998: Improving WSR-88D hourly rainfall estimates. *Wea. Forecasting,* **13,** 1016–1028.

Fulton, R. A., J. P. Breidenbach, D.-J. Seo, D. A. Miller, and T. O'Bannon, 1998: The WSR-88D rainfall algorithm. *Wea. Forecasting,* **13,** 377–395.

Joss, J., and R. Lee, 1995: The application of radar–gauge comparisons to operational precipitation profile corrections. *J. Appl. Meteor.,* **34,** 2612–2639.

Klazura, G. E., J. Thomale, D. Kelly, and P. Jendrowski, 1999: A comparison of NEXRAD WSR-88D rain estimates with gauge measurements for high and low reflectivity gradient precipitation events. Preprints, *29th Int. Conf. on Radar Meteorology,* Montreal, PQ, Canada, Amer. Meteor. Soc., 722–725.

McGregor, K. C., R. L. Bingner, A. J. Bowie, and G. R. Foster, 1995: Erosivity index values for northern Mississippi. *Trans. ASCE,* **38,** 1039–1047.

——, cited 1999: NWSRFS user's manual documentation. [Available

online at http://hsp.nws.noaa.gov/oh/hrl/nwsrfs/users_manual/htm/xrfsdochtm.htm.]

Seo, D.-J., 1998a: Real-time estimation of rainfall fields using rain gauge data under fractional coverage conditions. *J. Hydrol.,* **208,** 25–36.

——, 1998b: Real-time estimation of rainfall fields using radar rainfall and rain gauge data. *J. Hydrol.,* **208,** 37–52.

——, and J. A. Smith, 1996: Characterization of climotological variability of mean areal rainfall through fractional coverage. *Water Resour. Res.,* **33,** 2087–2095.

——, J. P. Briedenbach, and E. R. Johnson, 1999: Real-time estimation of mean field bias in radar rainfall data. *J. Hydrol.,* **223,** 131–147.

——, ——, R. Fulton, D. Miller, and T. O'Bannon, 2000: Real-time adjustment of range-dependent biases in WSR-88D rainfall estimates due to nonuniform vertical profile of reflectivity. *J. Hydrometeor.,* **1,** 222–240.

Smith, J. A., D. J. Seo, M. L. Baeck, and M. Hudlow, 1996: An intercomparison study of NEXRAD precipitation estimates. *Water Resour. Res.,* **32,** 2035–2045.

Smith, M. B., and W. F. Krajewski, 1991: Estimation of the mean field bias of radar rainfall estimate. *J. Appl. Meteor.,* **30,** 397–412.

——, V. Koren, D. Johnson, and B. Finnerty, 1999: Distributed modeling: Phase 1 results. NOAA Tech. Rep. NWS 44, 235 pp. [Available from M. B. Smith, NWS Office of Hydrology, 1325 East–West Highway, Silver Spring, MD 20910.]

Stellman, K. M., H. E. Fuelberg, R. Garza, and M. Mullusky, 1999: Utilizing radar data to improve streamflow forecasts. Preprints, *29th Int. Conf. on Radar Meteorology,* Montreal, PQ, Canada, Amer. Meteor. Soc., 931–934.

Ulbrich, C. W., and L. G. Lee, 1999: Rainfall measurement error by WSR-88D radars due to variations in *Z–R* law parameters and the radar constant. *J. Atmos. Oceanic Technol.,* **16,** 1017–1024.

Viessman, W., and G. L. Lewis, 1996: *Introduction to Hydrology.* 4th ed. Harper-Collins, 760 pp.

Viginal, B., H. Andrieu, and J. D. Creutin, 1999: Identification of vertical profiles of reflectivity from volume scan radar data. *J. Appl. Meteor.,* **38,** 1214–1228.

Wilson, J. W., and E. A. Brandes, 1979: Radar measurement of rainfall—A summary. *Bull. Amer. Meteor. Soc.,* **60,** 1048–1058.

Woodley, W. L., A. R. Olsen, A. Herndon, and V. Wiggert, 1975: Comparison of gauge and radar methods of convective rain measurement. *J. Appl. Meteor.,* **14,** 909–928.

Young, C. B., B. R. Nelson, A. A. Bradley, J. A. Smith, C. D. Peters-Lidard, A. Kruger, and M. L. Baeck, 1999: An evaluation of NEXRAD precipitation estimates in complex terrain. *J. Geophys. Res.,* **104,** 19 691–19 703.